EVIDENCE FOR VOLCANISM ASSOCIATED WITH THE FRACTURE ANNULUS OF ARAMAITI CORONA, VENUS. M. B. Russell[1] and C. L. Johnson[1,2], [1]Planetary Science Institute, Tucson, AZ 85719, USA (mrussell@psi.edu; cjohnson@psi.edu) [2]Dept. of Earth, Ocean and Atmospheric Sciences, University of British Columbia, Vancouver, BC, V6T 1Z4, Canada.

Introduction: The volcano-tectonic properties of coronae on Venus offer an opportunity to probe both interior and surface processes. Recent studies suggest Aramaiti Corona is potentially young and active [1, 2]. A study of lithospheric flexure at Aramaiti showed substantially thinner lithosphere and correspondingly larger heat flows than the global average [3], with even higher values of heat flow inferred from a flexural study of a smaller volcanic construct, Narina Tholus, associated with the corona's western outer fracture annulus [2]. Modeling studies of magma ascent paths beneath volcanic loads indicate that in areas of low lithospheric thickness, flexural stresses can produce annular, narrow zones of ascent and annular edifice construction [4]. SAR images support this: numerous volcanic features are spatially associated with the quasi-circular fracture annuli of coronae. Coronae annuli, therefore, can provide enticing locations to look for indications of past or current volcanic activity to constrain the resurfacing history of Venus.

Here, we report further evidence for volcanism associated with the fracture annulus of Aramaiti Corona, through an investigation of the unusual morphology of the northern portion of the topographic fracture annulus [5], referred to hereafter as the NFA. We use Magellan Synthetic Aperture Radar (SAR) images and SAR stereo-derived topography.

Analysis and Description: High resolution stereo (~1 km horizontal and 50-100 m vertical resolution) [6] over the NFA of Aramaiti shows undulating along-strike topography (Fig. 1a). Three spatially distinct topographic highs, domelike in shape, are superposed on the topographic rim, following the strike of the annulus fractures. The two eastern highs rise steadily about 250 m above the existing topographic rim and descend over a horizontal distance of ~12 km (Fig. 1a). The relief of each undulation is significant with respect to the vertical precision of the stereo topography [6]. It is not possible to assess features further west because of the discontinuous stereo topography coverage (Fig. 1a). However, the gridded altimetry data [7] indicate little positive relief, consistent with the east-to-west trend seen in the stereo.

In addition to the undulating topography, an extensive blocky deposit outboard of, and concentric to, the fracture annulus is clearly visible in the SAR images. The deposit lies at the base of the corona topographic rim, extending over a radial distance of ~6 km.

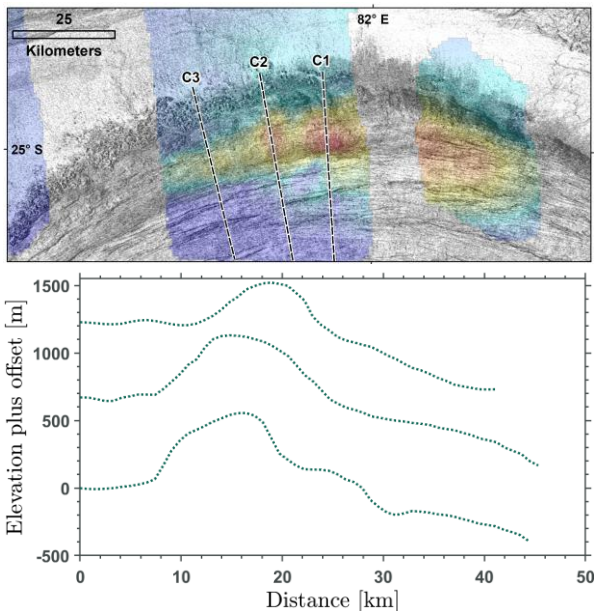

Fig. 1: (a) The northern fracture annulus of Aramaiti Corona. Inverted Magellan right-look SAR image superposed on stereo-SAR elevations (color). Elevation range is ~900 m from high (red) to low (blue). Dark shading in the SAR image represents radar bright. (b) Cross-strike profiles from north to south. From bottom to top these correspond to C1, C2, C3 in (a).

The material in the interior of the deposit is rough at the radar wavelength (12.6 cm), and contrasts with the underlying, radar-dark wrinkle-ridge plains [8] (Fig. 2). The western portion of the deposit appears to be composed of coherent, angular blocks with the radar-facing sides evidenced as bright (dark gray in the inverted images) linear features up to several hundred meters in length. Following the strike of the corona rim eastward, the radar signature of the deposit transitions from a blocky appearance to a more homogenous texture, indicating radar-bright material with a texture below the resolution of the radar. The outer boundary here has a 'wispy' appearance similar to those seen in the leeward side of some Venusian volcanic cones or impact crater parabolic ejecta blankets [9].

Mapping Material Boundaries: We used the automatic contour extraction tool in ArcGIS applied to the right-look SAR image to map units of differing texture and brightness within the deposit. We identified ~5 units with distinct textural properties (Fig. 2), visually corresponding to blockier vs finer textures. One

inner edge (S1 in Fig. 2) was mapped manually as there is insufficient contrast for it to be identified automatically.

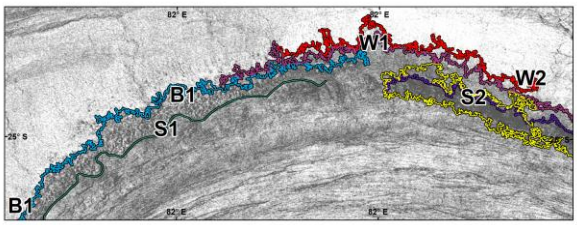

Fig. 2: NFA deposit with boundaries of distinct units mapped (see text). Main blocky boundary is labelled 'B1', boundaries of smoother materials, 'S' (S1, S1), and wispy boundaries with 'W' (W1, W2).

Mapping Radar-Bright Reflectors: We also mapped isolated radar-bright reflectors that extend radially beyond the crenulated edge of the deposit, which represent coherent blocks of material (either individual blocks or groups of blocks with sizes below the SAR image resolution). Their identification was possible because of the fortuitous contrast of the features with the underlying smooth unit (Fig. 2).

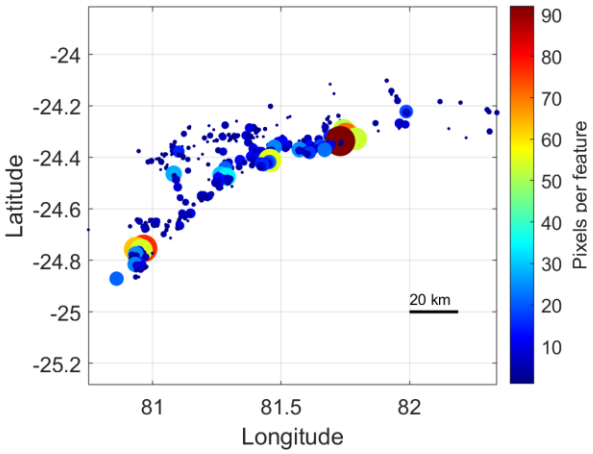

Fig. 3: Planform map of the block locations outboard of the NFA blocky deposit. Size and color represent block size (or collections of blocks so closely spaced that they appear as a single large feature).

The spatial density of blocks varies little with azimuth around the NFA, with little to no size sorting in this direction (Fig. 3). In the radial direction, both blocky and fine material emanate from the edge of the deposit as distinct trails. The larger blocks are generally proximal to the NFA, with relatively smaller blocks and finer material more distal. Isolated blocks are seen in the radial far-field, extending beyond the outer edge of main deposit (Fig. 3). The automatic mapping and contrast allowed the block sizes to be assessed, and most (70%) are one to four pixels in size, i.e., up to 75 – 300 m across.

Discussion: The irregular topography of the NFA is morphologically similar to volcanic domes on Earth such as the Ruawahia Dome in the Tarawera Volcanic Dome Complex in New Zealand. The hummocky texture of the aerially extensive deposit sitting at the base of the NFA, containing distinct blocks, is noted to occur on Earth associated with volcanic debris avalanches and used as a diagnostic on Venus to identify volcanic domes [10, 11]. These are proposed to be sourced from over-steepened portions of the volcanic edifice after most of the volcanic activity ceases [12]. The strength of the cooled material is high, but the over-steepened slopes can collapse catastrophically into large blocks (>1 km) and flows [10]. Another characteristic of volcanic domes, potentially relevant to the deposit at Aramaiti is talus [11, 14]. The absence of later embayment and fresh-looking morphology suggest that the deposit is stratigraphically younger and may be diagnostic of activity associated with late-stage evolution at a young corona [1]. At the very least, along part of the NFA, it is an example of mass movement associated with a steep slope, one key to understanding the current Venusian tectonic regime. Although there is evidence for blocky deposits associated with Venusian steep-sided domes, the combination of the planform of the deposit (annular rather than fan-like), the hummocky texture of the blocks and the fine deposits (W1, W2) associated with a corona rim is rare. We are conducting a systematic survey of Magellan stereo and SAR data for such expressions of volcanism around other coronae.

References: [1] Gülcher A.J.P. et al. (2020) *Nat. Geosci. 13*, 547-554. [2] Russell M.B. & Johnson C.L. (2021) *JGR Planets, 126,* e2020JE006783. [3] O'Rourke J.G. & Smrekar S.E. (2018) *JGR Planets, 123,* 369–389. [4] McGovern P.J. et al. (2013) *JGR Planets, 118*, 2423–2437. [5] Russell M.B. (2020) Univ. British Columbia. [6] Herrick R.R. (2020) NASA Planetary Data System. [7] Ford P.G. & Pettengill G.H. (1992) *JGR Planets, 97(E8),* 13103-13114. [8] Basilevsky A.T. & Head J.W. (1997) *Earth, Moon, and Planets 76*, 67–115. [9] Cohen-Zada A.L. et al. (2016) *Aeolian Research, 20*, 108-125. [10] López I. (2011) *Icarus, 213*(1), 73-85. [11] Siebert L. (1984) *J. Volcanology & Geothermal Research, 22* (3), 163-197. [12] Bulmer M.H. & Guest J.E. (1996) *GS Spec. Pub., 110,* 349–371. [13] Blake S. (1990) IAVCEI Proc. Volcanology, 88-126. [14] Fink J.H. & Griffiths R.W. (1998) *JGR Solid Earth*, 103(B1), 527- 545.